

# Data-Driven Models for Microscopic Vehicle Emissions

Hajar Hajmohammadi<sup>\*,a</sup>, Giampiero Marra<sup>b</sup>, Benjamin Heydecker<sup>a</sup>

<sup>a</sup> Centre for Transport Studies, Department of Civil, Environment and Geomatics Engineering,

University College London, Gower Street, London, WC1E 6BT, UK

<sup>b</sup> Department of Statistical Science, University College London, Gower Street, London, WC1E 6BT, UK

## Abstract

In this paper, a new approach for describing the relationship between tailpipe emissions and vehicle movement variables is presented, called generalized additive model for location, scale and shape (GAMLSS). The dataset for this model is second-by-second emission laboratory measurements, following a real driving cycle that were recorded in urban, suburban and motorway areas of London. The GAMLSS emission model is the model to estimate each of CO<sub>2</sub>, CO and NO<sub>x</sub> in each second for two different vehicle types (petrol or diesel) using instantaneous speed and acceleration as the explanatory variables. Comparing the results with current emission models indicates substantial improvement in accuracy and quality of estimation by this approach.

**Keywords:** vehicle emission modelling, GAMLSS approach, air pollution.

---

\* Corresponding author, E-mail: [Hajar.hosseinabadi.14@ucl.ac.uk](mailto:Hajar.hosseinabadi.14@ucl.ac.uk)

# 1. Introduction

Traffic management and control policies are generally developed to reduce traffic congestion, while their effects on the air pollution from road transport are not a main consideration. Vehicle emission modelling is an approach to estimate these effects on air quality. By using these models, traffic management policies can be developed considering vehicle emissions as well as other criteria.

Exhaust or tailpipe emission from road transport depends upon many factors that can be described as falling into two groups:

- Vehicle-related factors, such as model, engine size, fuel and catalyst type, mileage and technology level.
- Operational factors, such as driving style, road type and design, and traffic controls.

The focus of this paper is to introduce a predictive microscopic vehicle emission model that considers vehicle-related and operational factors. In this model, the nonlinear and intricate relationship between vehicle movement variables (speed and acceleration) and tailpipe emission ( $\text{CO}_2$ , CO and  $\text{NO}_x$ ) is described using a data-driven approach. This approach uses spline functions to capture as much information as possible from the explanatory variables without preconception of the form of the relationship as in parametric models. A consequence of this is that the model estimates emissions substantially better than generalized linear models (GLM), especially for the principal noxious emissions such as CO in the petrol and  $\text{NO}_x$  in the diesel vehicles. These pollutants are more complicated to estimate compared to  $\text{CO}_2$  because of the effects of catalyst and are important in the series of Euro standards that have become progressively more stringent since their introduction in 1992.

23 In this paper, two vehicle types (petrol and diesel) are selected to develop the model. The  
24 evaluation process shows that the goodness of fit (BIC) of the proposed model is substantially  
25 better than the parametric ones including classified log- polynomial regression and generalized  
26 linear model that are the basis of the CADI and GLM emission models, respectively. This  
27 improvement is more remarkable for CO estimation in the petrol and NO<sub>x</sub> in the diesel vehicles.

28 The paper is organized as follows: the background of the vehicle emission modelling is  
29 discussed in the next section, after which the dataset used for developing the proposed model  
30 is described in section 3. Section 4 is devoted to the methodology and model framework and  
31 after that the results are presented in section 5. The final section presents discussion and  
32 conclusions.

## 33 2. Background

34 A wide range of vehicle emission models have been developed up to now, mainly based on the  
35 type, amount and quality of available data. Type of explanatory variables and modelling  
36 approach of these models are discussed in this section.

### 37 2.1. Explanatory Variables

38 Burning fuel in the engine provides required power for vehicle movement, and fuel burning is  
39 the source of vehicle tailpipe emission. There are many factors from engine to the tailpipe that  
40 can affect the amount and type of emitted pollutants. The choice of explanatory variables to  
41 describe all these factors and engine mechanisms is a crucial part of a vehicle emission model.

42 The main explanatory variables for most microscopic emission models stem from the driving  
43 cycle or speed profile of the vehicle. These are instantaneous speed,  $v$ , and acceleration,  $a$ .

44 Another explanatory variable for emission modelling is engine power demand. Usually the

45 power per unit of mass or vehicle specific power ( $V$ ) is calculated from  $v$  and  $a$  to represent  
46 the engine power demand:

$$47 \quad V = \left( \frac{\alpha_1 + \alpha_2 v + \alpha_3 v^2}{M} + a + g \sin \theta \right) v, \quad (1)$$

48 where coefficients  $\alpha_1$ ,  $\alpha_2$  and  $\alpha_3$  represent rolling, rotating and drag resistance, respectively.  
49  $M$  is the mass,  $\theta$  is the road gradient and  $g$  is the acceleration due to gravity. This definition  
50 was first presented in [1] which was found to have strong correlation with vehicle emission.

51 Examples of using speed and acceleration for emission modelling are MODEM and DGV [2].  
52 These two models are similar in concept, both producing emission maps based on speed and  
53 acceleration. MODEM, produced during the European Commission's DRIVE research  
54 programme, uses two-dimensional look-up table for a particular vehicle type and pollutant  
55 according to the vehicle speed,  $v$ , and  $v \times a$ . The estimated mean rate of emissions is the  
56 arithmetic means of all observations in the cells, weighted according to their frequency in the  
57 driving cycle. The DGV model follows the same methodology, except the look-up table is  
58 formed by speed,  $v$ , and acceleration,  $a$ .

59 Vehicle specific power ( $V$ ) is a key contributing factor in the emission models such  
60 as MOVES2004, developed by Koupal et al. [3]. In this model, a unidimensional look-up table  
61 for emission (or fuel consumption) is indexed by values of  $V$ . The vehicle emission (or fuel  
62 consumption) is then estimated as the frequency- weighted arithmetic mean according to the  
63 driving cycle.

## 64 2.2. Modelling approach

65 Multiple linear, log-linear, log-polynomial and generalized linear model (GLM) are widely  
66 used in current emission models such as VERSIT+ [4], VT-micro [5-7] and EMIT [8].

67 VERSIT+ was developed by the Netherlands Organisation for Applied Scientific Research.  
68 This model uses speed as an explanatory variable and GLM regression approach to estimate  
69 emission for levels of local, regional and national for specific vehicle types. While VERSIT+  
70 uses a single model for the relationship between speed and tailpipe emission, other models such  
71 as VT-micro and CMEM<sup>1</sup> [9-11] implement classification based on the driving mode: Cruise,  
72 Accelerate, Decelerate, Idle (CADI), to improve undifferentiated models. The Virginia Tech  
73 microscopic model or VT-micro uses a classified log-polynomial model based on speed,  $v$ ,  
74 and acceleration,  $a$ :

$$75 \quad E = \begin{cases} \exp\left(\sum_{i=0}^3 \sum_{j=0}^3 \alpha_{i,j} v^i a^j\right) & (a \geq 0) \\ \exp\left(\sum_{i=0}^3 \sum_{j=0}^3 \beta_{i,j} v^i a^j\right) & (a < 0), \end{cases} \quad (2)$$

76 where  $E$  is tailpipe emission,  $v$  is vehicle speed with exponent  $i$  ( $0 \leq i \leq 3$ ),  $a$  is acceleration  
77 with exponent  $j$  ( $0 \leq j \leq 3$ ), and  $\alpha$  and  $\beta$  are the model coefficients for acceleration and  
78 deceleration, respectively.

79 In this classification, deceleration mode is identified by  $a < 0$  whilst the other CADI modes  
80 are merged into the  $a \geq 0$  case. For a complete CADI classification, speed should be involved  
81 ( $a \approx 0$  and  $v > 0$  for cruising and  $a = 0$ ,  $v = 0$  for idling). In the CMEM, each CADI operating  
82 mode is considered separately to estimate exhaust emission and fuel consumption. This model  
83 first estimates engine-out emission ( $E^o$ ) based on vehicle specific power,  $V$ , then the tailpipe  
84 emission is calculated as a function of engine-out emission, fuel consumption rate and catalyst  
85 pass fraction.

---

<sup>1</sup>-Comprehensive Modal Emissions Model

86 EMIssions from Traffic or EMIT is another classified model for estimating vehicle emission  
87 and fuel consumption of light duty vehicles [8]. The form of this model for estimating  $E^o$  from  
88 speed and acceleration is the classified polynomial form:

$$89 \quad E^o = \begin{cases} \omega_0 + \omega_1 v + \omega_2 v^2 + \omega_3 v^3 + \omega_4 va & (V > 0) \\ \omega'_0 & (V = 0) \end{cases} \quad (3)$$

90 where  $\omega$  is the model coefficient are the model coefficients, and  $V$  is the vehicle specific  
91 power.

92 This corresponds to classification according to vehicle specific power rather than acceleration.  
93 In terms of explanatory variables, the focus of the present study is to identify a simple set of  
94 variables based on the driving cycle to estimate tailpipe emission. Separate estimation of  
95 engine-out and tailpipe emission such as CMEM and EMIT increases the number of parameters  
96 required and adds extra complexity to the model, so is avoided here. This study proposes a  
97 model in the form of a single versatile model, using data-driven approach, rather than a  
98 parametric classified one such as VT-micro.

### 99 3. Dataset

100 The data used in the present study were generated in laboratory emission tests that were  
101 performed by Millbrook Laboratory using a chassis dynamometer, a full-scale dilution tunnel,  
102 and exhaust gas analysers. The chassis dynamometer should be capable of simulating the  
103 transient inertial load, aerodynamic drag and rolling resistance associated with normal  
104 operations of the vehicle [12] within a static laboratory.

#### 105 3.1. Real London driving cycle

106 Vehicle emission tests are performed based on a driving cycle or a time series of vehicle speed,  
107 that are sometimes intended to represent more or less typical driving patterns. A visual display

108 of the desired and actual vehicle speed is provided for the driver, so they can follow the  
109 prescribed driving cycle. For this study, real driving cycle data were logged second-by-second  
110 during three separate drives on certain routes in London (Figure 1) on each of two days to allow  
111 for an averaging effect in case of any atypical traffic conditions encountered. The recorded data  
112 were then used as the target driving cycles in the laboratory emissions measurements. A total  
113 of 9 real driving cycles were defined according to the type of the road (urban, suburban and  
114 motorway), and traffic conditions (AM peak, inter peak and free flow) for the emission tests.  
115 In Table 1 statistical information of the real driving cycles is summarized. The driving cycle  
116 of free flow in urban, suburban and motorway is shown in Figure 2.

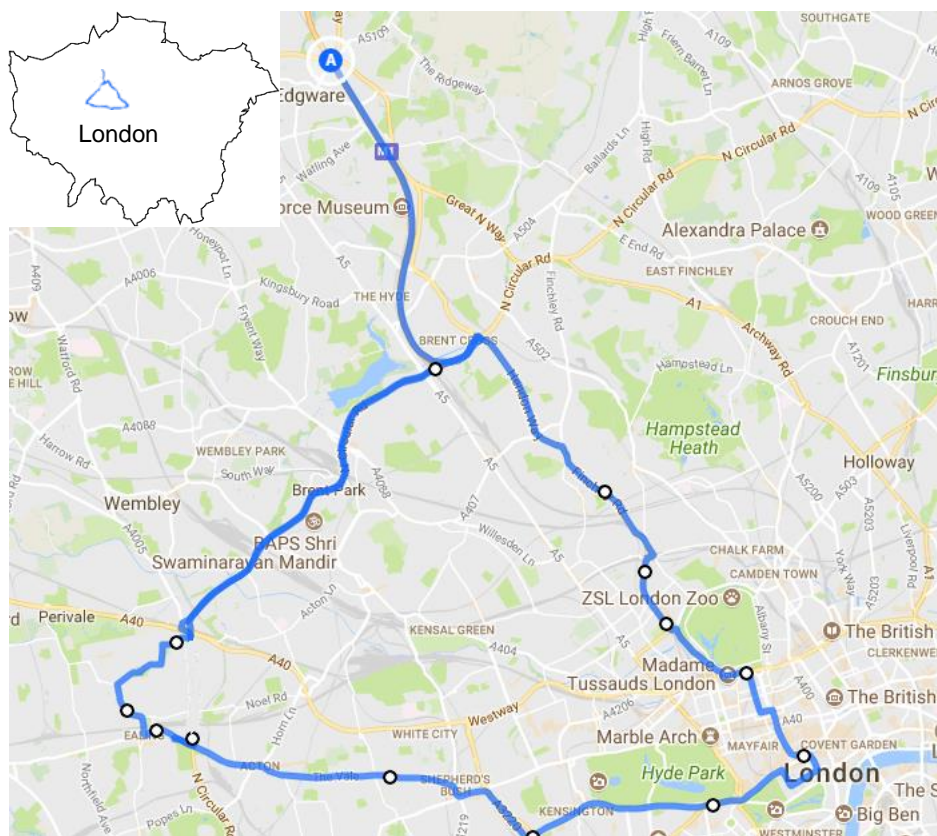


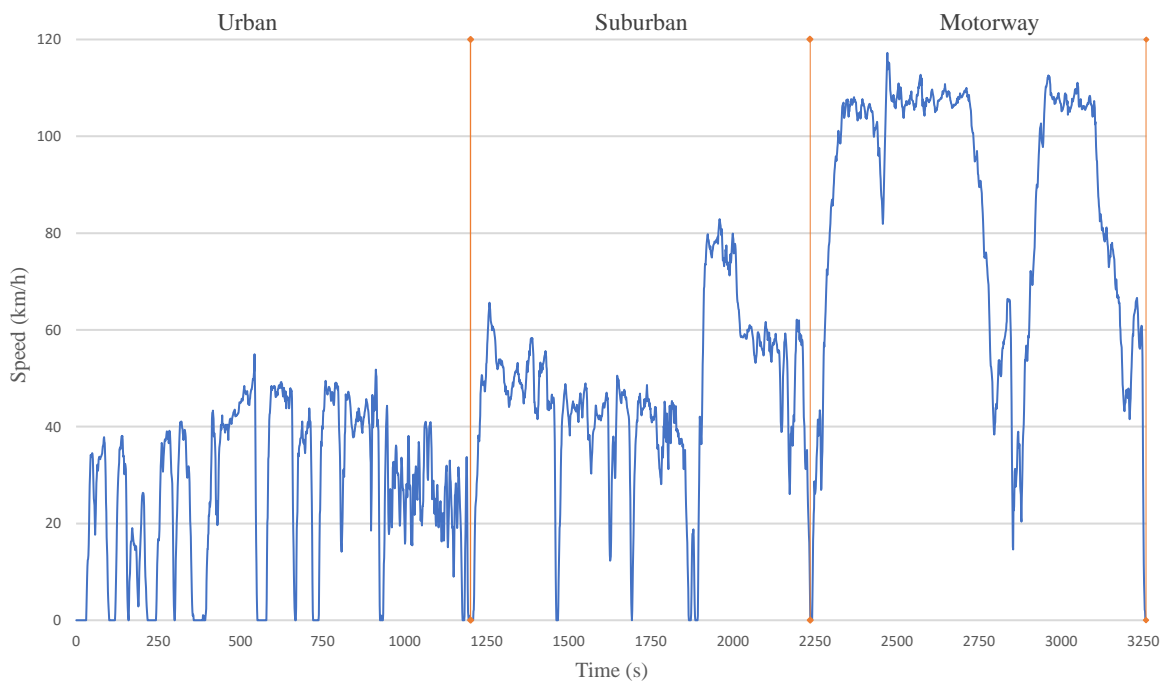
Figure 1: Map illustrating the route for data logging

135

Table 1: statistical information of the real driving cycles

	Average speed (km/h)	Maximum speed (km/h)	Std. Dev. speed (km/h)	Maximum acceleration (m/s <sup>2</sup> )	Minimum acceleration (m/s <sup>2</sup> )	Std. Dev. acceleration (m/s)	Duration (sec)	Length (km)
<b>Urban</b>								
Free Flow	26.53	52.85	16.24	1.91	-2.87	0.63	1202	8.86
AM peak	15.57	50.79	15.31	1.78	-2.43	0.58	2048	
Inter peak	13.80	49.48	14.58	2.36	-2.85	0.56	2310	
<b>Suburban</b>								
Free Flow	46.04	82.53	16.94	2.06	-2.92	0.49	1036	13.25
AM peak	25.15	78.42	22.06	2.36	-2.62	0.57	1867	
Inter peak	30.13	80.65	23.27	2.1	-2.64	0.57	1597	
<b>Motorway</b>								
Free Flow	86.18	113.32	27.21	1.69	-3.09	0.41	1025	24.54
AM peak	46.84	113.94	39.60	1.93	-2.72	0.51	1884	
Inter peak	85.77	113.03	31.75	2.21	-2.43	0.41	1030	

136



137

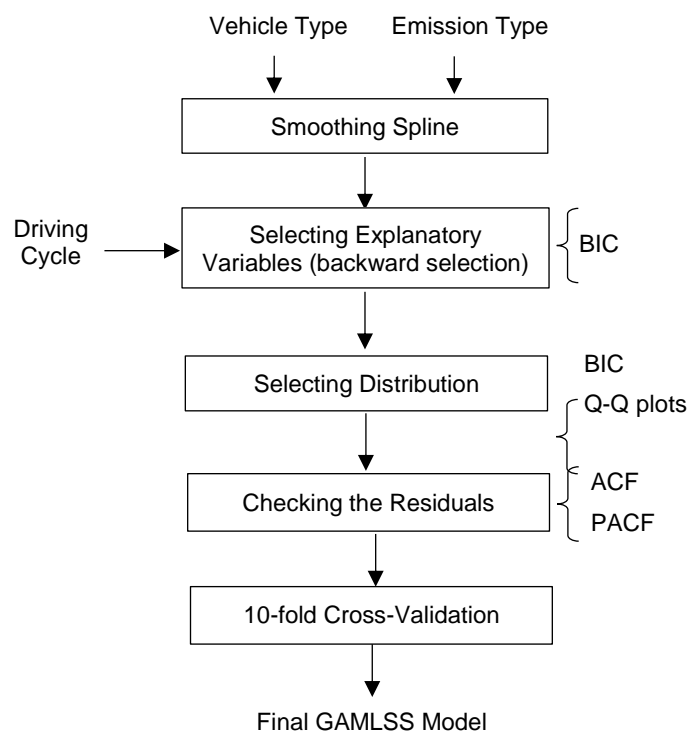
138

Figure 2: real driving cycle for urban, suburban and motorway, free flow traffic conditions



## 139 4. Model framework

140 The present emission model is a Generalized Additive Model for Location, Scale and Shape  
141 (GAMLSS) [13, 14], that is an extended class of generalized additive model (GAM) [15]. An  
142 outline of the model building process is shown in Figure 3. The calculations presented here  
143 were undertaken using the model as implemented in the GJMR [16, 17] R package (version 2).  
144 The R codes used for this study are presented in Appendix. The components of this model are  
145 explained in the following.



158 *Figure 3: GAMLSS model building process*

### 159 4.1. Spline smoothing function

160 A smooth function is adopted to summarize the trend of a response variable in respect of one  
161 or more explanatory variables. It is formed piecewise of polynomial (of order  $M$ ) sections that  
162 are  $M - 1$  times continuously differentiable at the joints, resulting in a smooth function that  
163 can follow relationships in the data.

164 The method of splines, as applied in this paper, consists of dividing up the range of each  
 165 explanatory variable  $x$  into segments with join points at the boundaries which are known as  
 166 knots. A polynomial of a fixed degree is then fitted to the observed values of the response  
 167 variable within each segment with constraints applied at the knots to ensure appropriate  
 168 continuity there. Hence, the spline function  $s(x)$  of order  $M$  (degree  $M - 1$ ) with knots at  
 169  $x = \xi_1, \dots, \xi_K$  (where  $\xi_1 < \xi_2 < \dots < \xi_K$ ) and a domain  $[a, b]$ , is defined as a function with the  
 170 following properties:

171 1) In each of the intervals:

172  $a < x < \xi_1$ ,  $\xi_{j-1} \leq x \leq \xi_j$  ( $j = 2, 3, \dots, K$ ), and  $\xi_K \leq x \leq b$ ,  $s(x)$  is a polynomial of degree  
 173  $M - 1$  at most.

174 2)  $s(x)$  and its derivatives up to order  $M - 2$  are continuous at each of the knots.

175 The univariate spline of order  $M$ ,  $s_M(\cdot)$ , can be represented analytically in the form:

$$176 \quad s_M(x) = \sum_{h=0}^{M-1} \alpha_h x^h + \sum_{j=1}^K \beta_j (x - \xi_j)_+^{M-1},$$

$$177 \quad \text{where } u_+ = \begin{cases} u & (u \geq 0) \\ 0 & (u \leq 0). \end{cases} \quad (4)$$

178 This shows clearly the continuity of derivatives up to  $M - 2$  at all values of the explanatory  
 179 variable  $x$ , including the knots. However, other representations are better conditions for  
 180 computation, and so are preferred for that. Duchon [18] extended this approach to one or more  
 181 dimensions of explanatory variables, which is known as thin plate regression splines (TPRS).

182 A penalized maximum likelihood criterion is then used for fitting the TPRS,  $s_{tp}$ , by solving the  
 183 joint optimisations:

$$\lambda^* = \arg \min_{\lambda} A(\lambda) = -2\mathcal{L}(\boldsymbol{\alpha}_{\lambda}, \boldsymbol{\beta}_{\lambda} | \mathbf{x}) + 2e(\boldsymbol{\alpha}_{\lambda}, \boldsymbol{\beta}_{\lambda}, \lambda)$$

184 where, (5)

$$\boldsymbol{\alpha}_{\lambda}, \boldsymbol{\beta}_{\lambda} = \arg \min_{\boldsymbol{\alpha}, \boldsymbol{\beta}} B(\boldsymbol{\alpha}, \boldsymbol{\beta}) = -\mathcal{L}(\boldsymbol{\alpha}, \boldsymbol{\beta} | \mathbf{x}) + \lambda J_p(s_{ip}(\boldsymbol{\alpha}, \boldsymbol{\beta}))$$

185 where  $\mathcal{L}(\cdot)$  is the log-likelihood of the spline,  $J_p(\cdot)$  is a penalty function for roughness of the  
 186 spline, and  $e(\cdot)$  is the effective degrees of freedom of the spline (Wood, 2017, p269). The first  
 187 line corresponds to a performance optimisation to determine the value of the smoothing  
 188 parameter  $\lambda$  that optimises the Akaike information criterion  $A(\cdot)$  of the fitted model with  
 189 effective degrees of freedom  $e$  while the second line determines the associated model  
 190 parameters  $\boldsymbol{\alpha}_{\lambda}, \boldsymbol{\beta}_{\lambda}$  that optimise the  $\lambda$ -penalised likelihood  $B$ .

191 The penalty function for a TPRS with one explanatory variable and 2 continuous derivatives  
 192 is defined by:

$$193 \quad J_{p,1} = \int_a^b [s''_{ip}(x)]^2 dx. \quad (6)$$

194 And the penalty function for  $s_{ip}$  with two explanatory variables is:

$$195 \quad J_{p,2} = \iint \left( \frac{\partial^2 s_{ip}}{\partial x_1^2} \right)^2 + 2 \left( \frac{\partial^2 s_{ip}}{\partial x_1 \partial x_2} \right)^2 + \left( \frac{\partial^2 s_{ip}}{\partial x_2^2} \right)^2 dx_1 dx_2 \quad (7)$$

196 The effect of the smoothing parameter is to reduce the curvature of the spline function, with a  
 197 consequent reduction in the effective degrees of freedom  $e$  corresponding to the number of  
 198 free parameters in the model: without this, use of the maximal set of knots would lead to an  
 199 underspecified spline function with a potentially high degree of roughness.

## 200 [4.2. Selecting explanatory variables](#)

201 The driving cycle is the source of explanatory variables for the present emission models. In  
 202 order to develop the model, the initial set of explanatory variables was selected as:

203  $\mathbf{x} = [v \ v^2 \ v^3 \ a \ av]^T$ . These explanatory variables represent the physical concept of  
204 vehicle specific power (  $V$  ) components from equation 1:

- 205 • Power to accelerate:  $av$
- 206 • Rolling resistance:  $v$
- 207 • Rotating resistance:  $v^2$
- 208 • Air resistance:  $v^3$

209 The model initially was run using all of these variables, and then variables were considered for  
210 elimination according to the backward selection procedure. The Bayesian Information  
211 Criterion (BIC) was used to assess model performance at each stage:

$$212 \quad BIC = -2\mathcal{L} + \log_e(n)p \quad (8)$$

213 where  $p$  is the effective degrees of freedom, corresponding to the number of free parameters  
214 in the model,  $n$  is the number of observations and  $\mathcal{L}$  is the log-likelihood of the model.  
215 Models with smaller values of BIC are preferred: this provides a balance between lack of fit  
216 (represents by lower log-likelihood) and model complexity (represented by the number  $p$  of  
217 parameters used). This criterion penalizes additional parameters according to the number  $n$  of  
218 observations used to fit the model. Whenever  $n \geq 8 \approx e^2$  the entry criterion for additional  
219 parameters is more stringent than that of Akaike's information criterion  $AIC = -2\mathcal{L} + 2p$ , thus  
220 leading to less complicated models.

221 By applying this process, the final explanatory variables in the model were selected as:  
222 speed ( $v$ ), acceleration ( $a$ ) and their product ( $va$ ). Other variables were eliminated from the  
223 model as they could not be justified as efficient in improving the estimation based on the BIC  
224 values.

225 The resulting emission models for two different vehicle types. The characteristics of these  
 226 vehicles are presented in Table 2.

227 *Table 2: Characteristics of tested vehicles*

code	Type	Fuel	Transmission	Engine size (cc)	Mass (kg)
A	Compact	Petrol	Manual	1000	900
B	Supermini	Diesel	Manual	1400	1200

### 231 4.3. GAMLSS emission model

232 GAM models explained the relationship between response and explanatory variables only in  
 233 terms of smooth functions, rather than the more limited specified parametric regressions, such  
 234 as Genrelized Linear Model (GLM). The extended class of GAM is introduced by Rigby and  
 235 Stasinopoulos [19] as the general additive model for location, scale and shape, GAMLSS. the  
 236 model has three components:

- 237 1) Systematic component, that contains smooth functions of explanatory variables
- 238 2) Response variable distribution or error structure
- 239 3) Link function, that connect the parameters of the response variable distribution to the  
 240 systematic component

241 By extension to GAM, in GAMLSS the outcome distribution is not restricted to belong to the  
 242 exponential family. The systematic part of the GAMLSS is expanded to allow modelling of not  
 243 only the mean (or location) but also the other parameters (scale and shape) of the response  
 244 variable distribution. The systematic part of the GAMLSS emission model is the sum of splines  
 245 of the explanatory variables (hence the epithet “additive”):

$$246 \quad \eta_{i,j} = S_{\eta 1_j}(v_i) + S_{\eta 2_j}(a_i) + S_{\eta 3_j}(v_i, a_i) \quad (9)$$

247 where  $\eta_{i,j}$  is the systematic component of observation  $i$  for estimating parameter  $j$  of the  
 248 statistical distribution.

249 For each emission type, the GAMLSS emission models were tested by using twelve possible  
 250 one, two and three-parameter distributions, presented in detail in [14]. The BIC values of the  
 251 models, as well as the Q-Q (quantile-quantile) plots of normalized quantile residuals were used  
 252 to assess the goodness of fit of the models according to each of these distributions.

253 According to this process, two distributions were identified for emission modelling: Fisk and  
 254 the extended version of that, Dagum. These are defined as follows:

255 Fisk distribution:

$$256 \quad f(y; \mu, \sigma) = \frac{\sigma y^{\sigma-1}}{\mu^\sigma \left[ 1 + \left( \frac{y}{\mu} \right)^\sigma \right]^2} \quad (10)$$

257 for  $y > 0, \mu > 0, \sigma > 0$ .

258 For moment  $k$  of this distribution to exist, the parameter  $\sigma$  is restricted as  $\sigma > k$ . Subject to  
 259  $\sigma > 2$ , the first and second moments are:

$$260 \quad E(Y) = \frac{\mu\pi/\sigma}{\sin(\pi/\sigma)} \quad \text{and} \quad \text{VAR}(Y) = \mu^2 \left[ \frac{2\pi/\sigma}{\sin(2\pi/\sigma)} - \left( \frac{\pi/\sigma}{\sin(\pi/\sigma)} \right)^2 \right].$$

261 The Dagum distribution is:

$$262 \quad f(y; \mu, \sigma, \nu) = \frac{\sigma\nu}{y} \left[ \frac{\left( \frac{y}{\mu} \right)^{\sigma\nu}}{\left[ 1 + \left( \frac{y}{\mu} \right)^\sigma \right]^{\nu+1}} \right], \quad (11)$$

263 for  $y > 0$  and location, scale and shape parameters, respectively  $\mu > 0, \sigma > 0, \nu > 0$ .

264 Provided that  $\sigma > 2$ , the first and second moments are:

$$E(Y) = \frac{-\mu \Gamma\left(\frac{-1}{\sigma}\right) \Gamma\left(\frac{1}{\sigma} + \nu\right)}{\sigma \Gamma(\nu)}, \text{Var}(Y) = -\left(\frac{\mu}{\sigma}\right)^2 \left[ 2\sigma \frac{\Gamma\left(\frac{-2}{\sigma}\right) \Gamma\left(\frac{2}{\sigma} + \nu\right)}{\Gamma(\nu)} + \left(\frac{\Gamma\left(\frac{-1}{\sigma}\right) \Gamma\left(\frac{1}{\sigma} + \nu\right)}{\Gamma(\nu)}\right)^2 \right].$$

Based on the range of the  $y$  in both Fisk and Dagum distribution, the link function for all their parameters is the logarithm. Hence, the GAMLSS models for each of the different emittants have distributions with parameters defined by:

for the Fisk distribution model:

$$\mu_i = \exp \eta_{i,1}, \sigma_i = \exp \eta_{i,2} \quad (12)$$

and for the Dagum distribution model:

$$\mu_i = \exp \eta_{i,1}, \sigma_i = \exp \eta_{i,2}, \nu_i = \exp \eta_{i,3}. \quad (13)$$

## 5. Results

The results of estimation, evaluation and cross validation of the GAMLSS emission model is presented in this section. The results are presented for each vehicle type (A and B) and emission type (CO<sub>2</sub>, CO and NO<sub>x</sub>) separately.

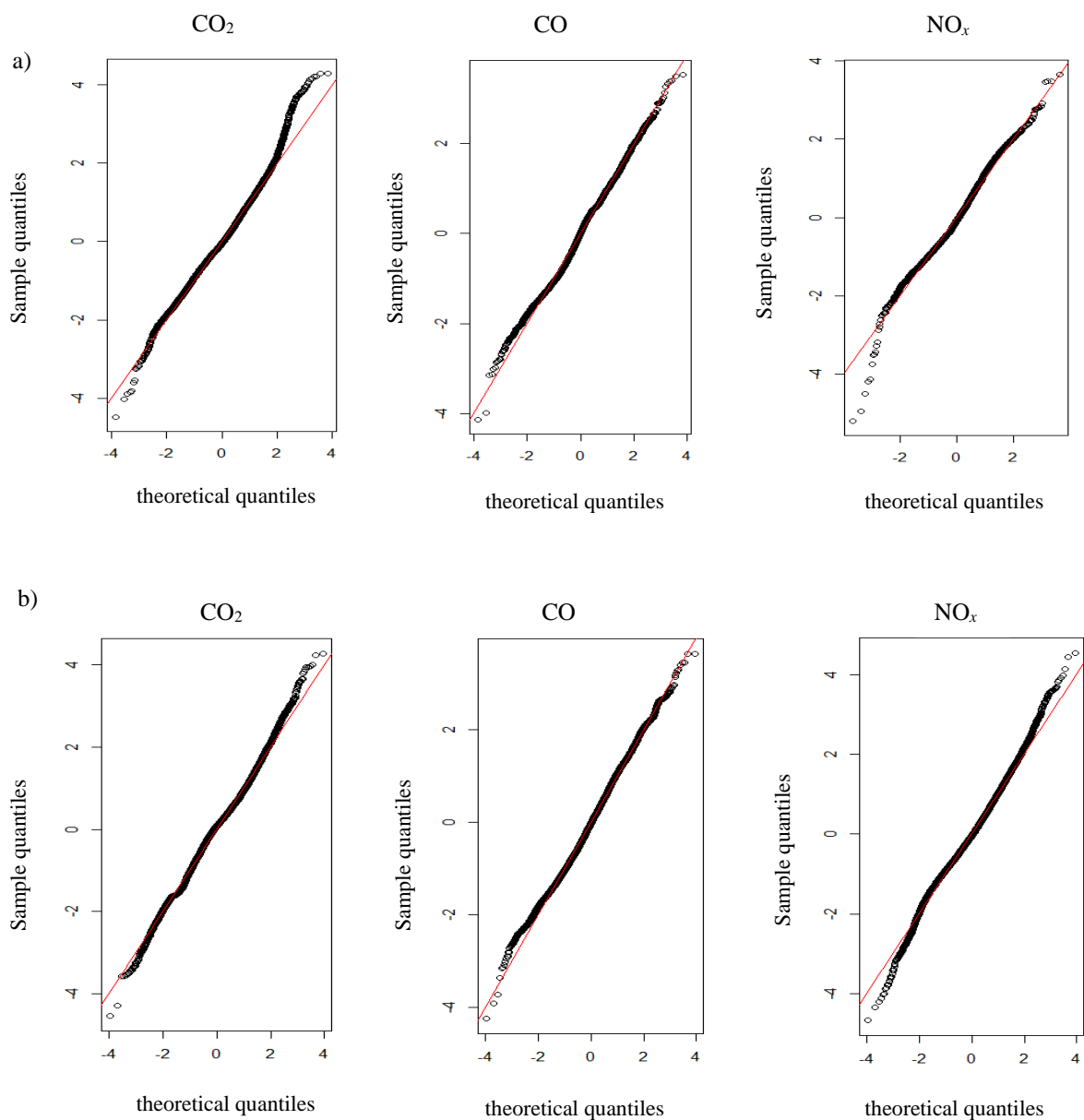
### 5.1. Fitted distributions

According to the process described in section 4.3, twelve possible distributions were fitted to the emission and the best distribution selected according to the BIC values and Q-Q plots of normalized quantile residuals (Table 3). The Q-Q plots of fitted distribution are presented in Figure 4.

282 In these plots, sample quantiles are the emission observation ( $\text{CO}_2$ , CO and  $\text{NO}_x$ ) and the  
 283 theoretical quantiles are calculated from the selected distributions. The reference red line  
 284 indicates the case in which the both quantiles are from the same distribution.

285 *Table 3: Results of distribution selecting for each vehicle type and emission type*

	Selected Distribution		
	$\text{CO}_2$	CO	$\text{NO}_x$
Vehicle A	Fisk	Fisk	Dagum
Vehicle B	Dagum	Dagum	Fisk



311 *Figure 4 : analysis of quantile residuals for a) vehicle 1 and b) vehicle 2*



312 5.2. Estimation

313 For each vehicle and emission type, GAMLSS approach (models (12) and (13)) were applied  
314 to the dataset. The results are presented in Figure 5- Figure 10.

315 Plot (a) in these figures is the smooth function of speed,  $S_{p1}(v)$ , plot (b) is the smooth function  
316 of acceleration,  $S_{p2}(a)$ , and plot (c) is the interaction of speed and acceleration,  $S_{p3}(v \times a)$ .

317 The shape of smooth functions for petrol (A) and diesel (B) vehicle types are different in most  
318 cases. In vehicle A,  $S_{p1}(v)$  approximately has a constant positive slop particularly when  $v \geq 60$   
319 km/h for CO<sub>2</sub>. This increasing trend is repeated for CO, with a constant positive slop for  
320  $10 \leq v \leq 40$ km/h. For NO<sub>x</sub>, the smooth function of speed has approximately no effect on the  
321 emission for  $20 \leq v \leq 60$  km/h, and after that it has an increasing trend with a limited slop. The  
322 reason of that comes from low variation in the NO<sub>x</sub> values in the petrol vehicle.

323 The smooth function of speed for vehicle B can be divided into four categories. Decreasing  
324 trend for  $v \leq 20$ km/h, increasing trend for  $20 \leq v \leq 40$  km/h, decreasing trend for  $40 \leq v \leq 60$   
325 and increasing trend for  $v \geq 60$ . These fluctuations for speed is approximately repeated for  
326 CO<sub>2</sub>, CO and NO<sub>x</sub>, with little differences in CO.

327 The smooth function of acceleration,  $S_{p2}(a)$ , has a changing point close to the  $a \approx 0$  m/s<sup>2</sup> for  
328 some of the emission types. That could be interpreted as the different effects of  $S_{p2}(a)$  on the  
329 emission in acceleration and deceleration driving modes. Smooth functions of acceleration for  
330 CO in vehicle B and NO<sub>x</sub> in vehicle A have limited effects on the emission, due to the low  
331 variations of CO and NO<sub>x</sub> in the diesel and petrol vehicles, respectively. For other emission  
332 types, the increasing trend when  $a < 0$  m/s<sup>2</sup> and then decreasing trend when  $a$  is positive can  
333 be observed for vehicle B.

334 The highest effect of interaction between speed and acceleration on CO<sub>2</sub> and CO for vehicle A  
335 is when  $40 \leq v \leq 60$  km/h and  $-3.5 \leq a \leq 2.5$  m/s<sup>2</sup> (medium speed and harsh deceleration). For  
336 NO<sub>x</sub>, it is when the speed is low ( $v \approx 20$  km/h) and  $-2 \leq a \leq -1$  m/s<sup>2</sup> (deceleration). For vehicle  
337 B, the highest impacts of interaction on CO and NO<sub>x</sub> is when  $v \leq 20$  km/h (low speed) and  
338  $a \approx -3$  m/s<sup>2</sup> (harsh deceleration). For CO<sub>2</sub> of this vehicle, the interaction effects is high when  
339  $40 \leq v \leq 80$  km/h (medium speed) and  $a \leq -1$  m/s<sup>2</sup> (deceleration).

340

341

342

343

344

345

346

347

348

349

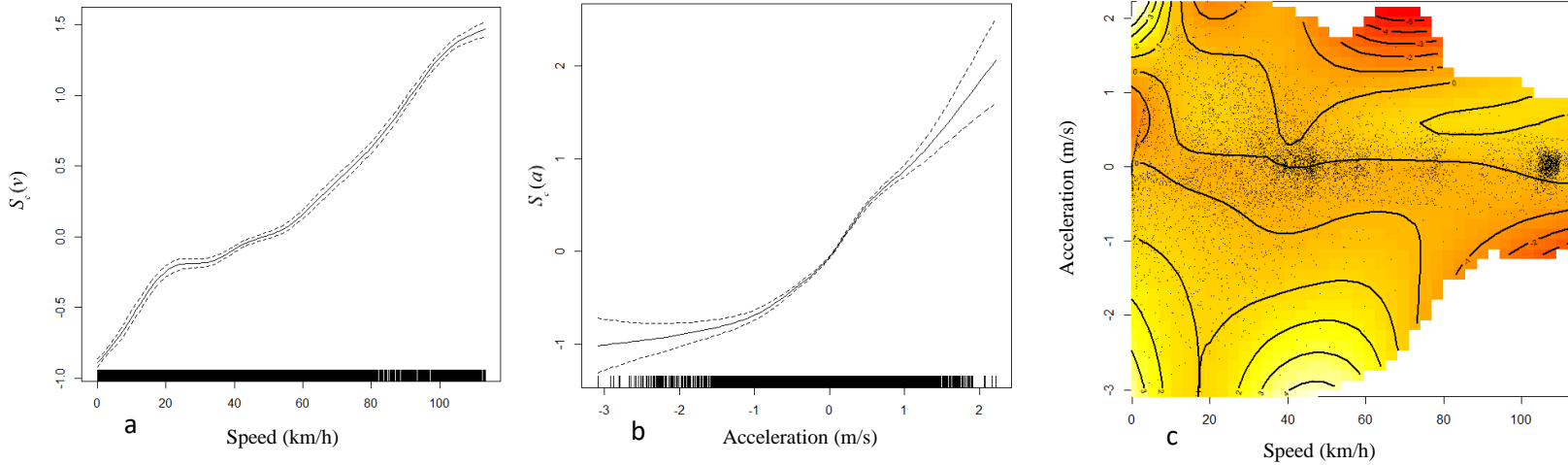


Figure 5: CO<sub>2</sub>, vehicle A: a) smooth function of speed, b) smooth function of acceleration and c) smooth function of interaction between speed and acceleration

350

351

352

353

354

355

356

357

358

359

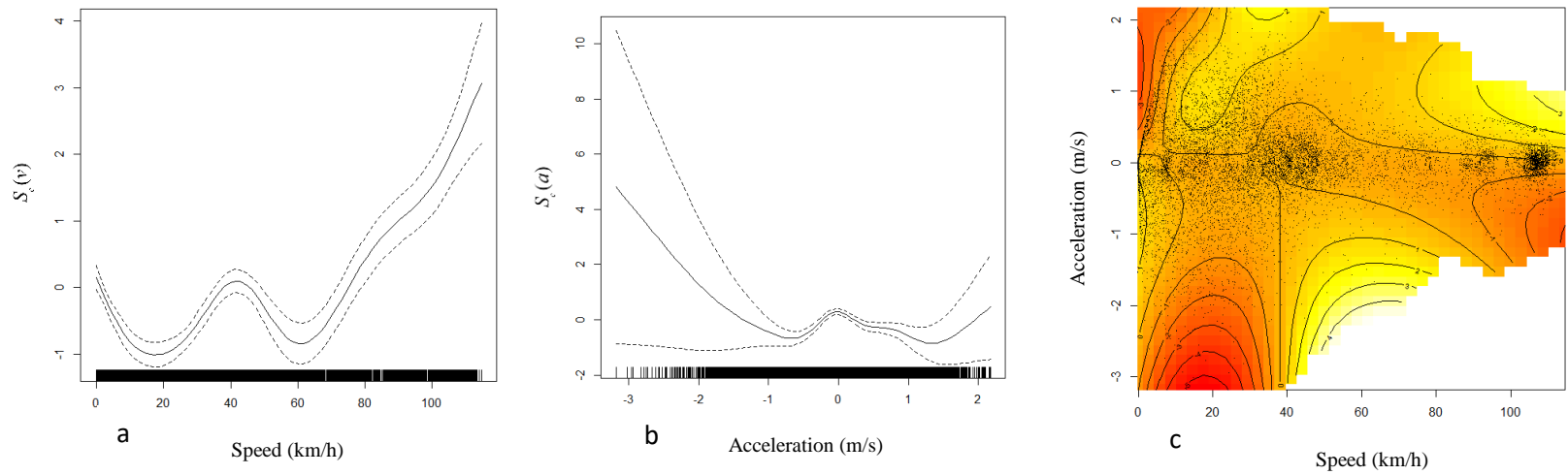


Figure 6: CO<sub>2</sub>, vehicle B: a) smooth function of speed, b) smooth function of acceleration and c) smooth function of interaction between speed and acceleration

361

362  
363  
364  
365  
366  
367  
368  
369  
370  
371  
372  
373  
374  
375  
376  
377  
378  
379  
380  
381  
382

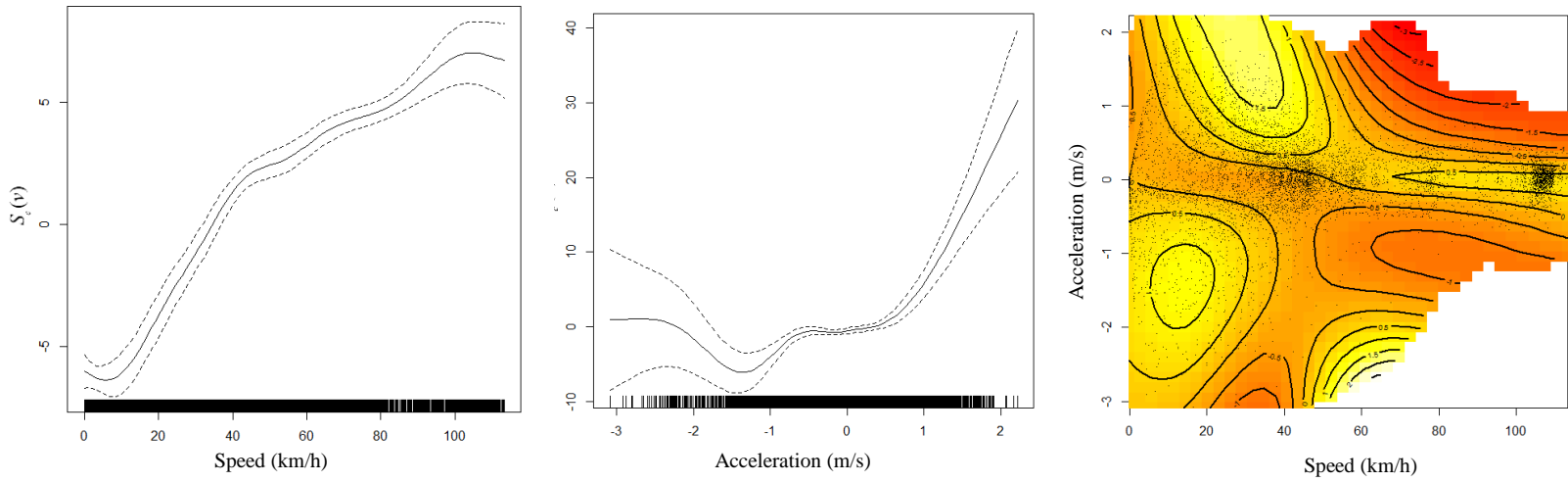


Figure 7: CO, vehicle A: a) smooth function of speed, b) smooth function of acceleration and c) smooth function of interaction between speed and acceleration

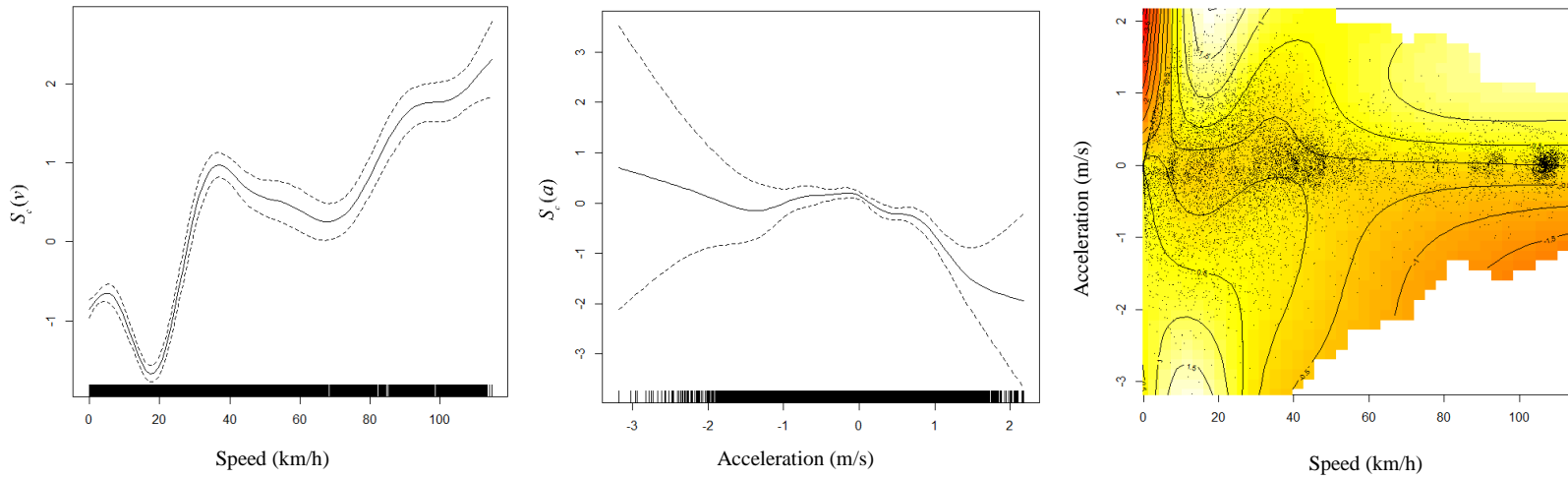
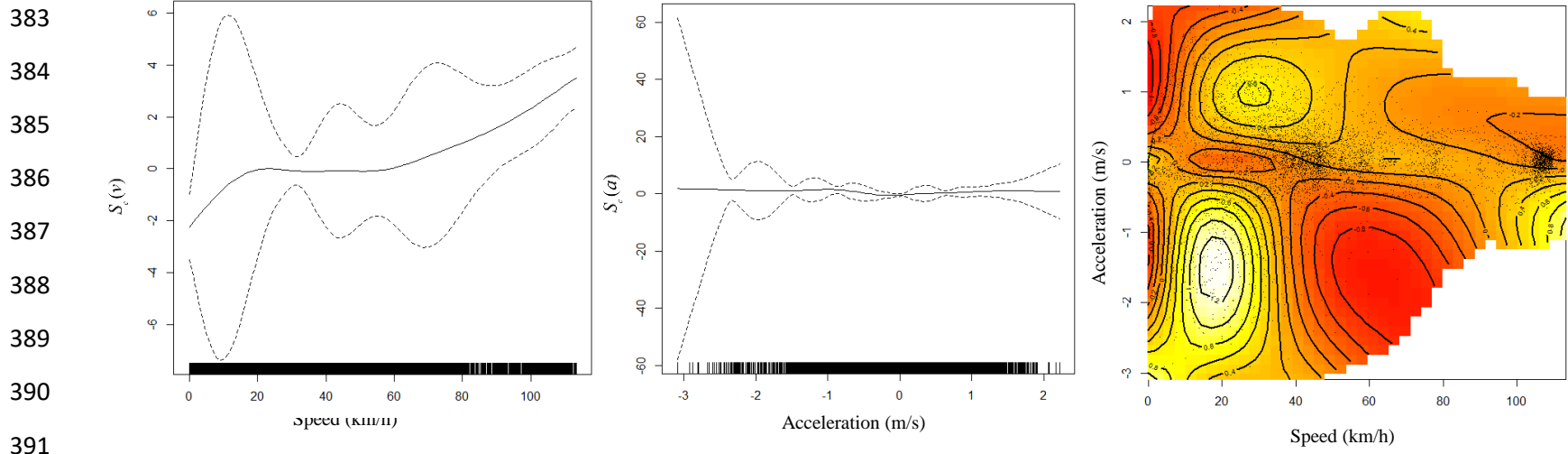
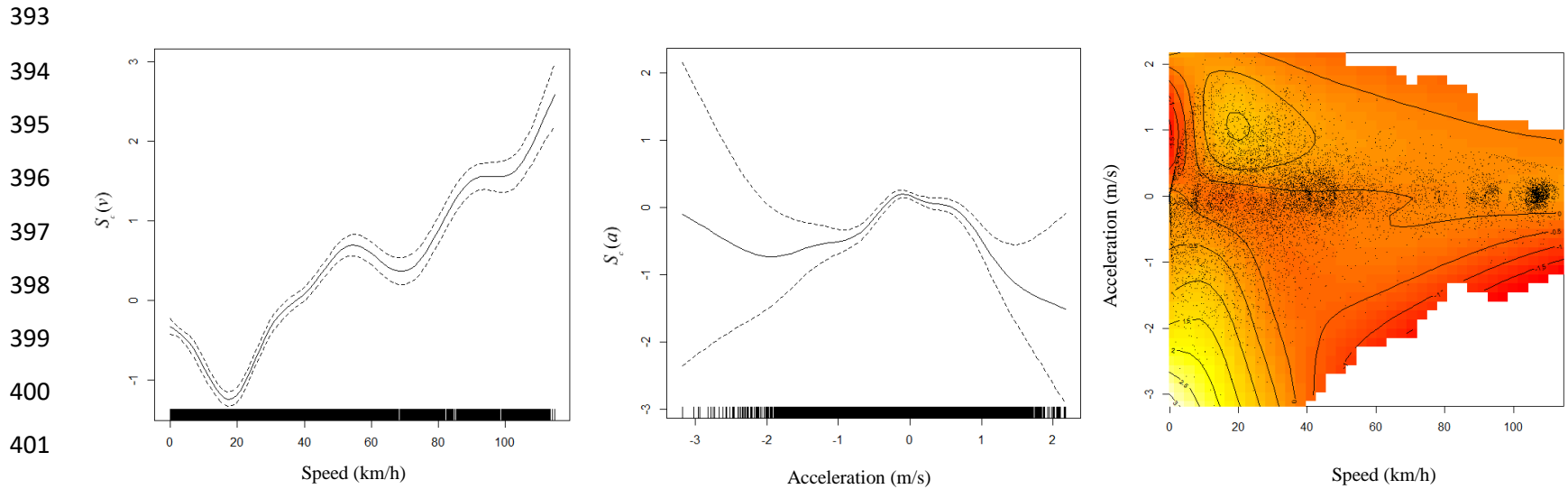


Figure 8: CO, vehicle B: a) smooth function of speed, b) smooth function of acceleration and c) smooth function of interaction between speed and acceleration



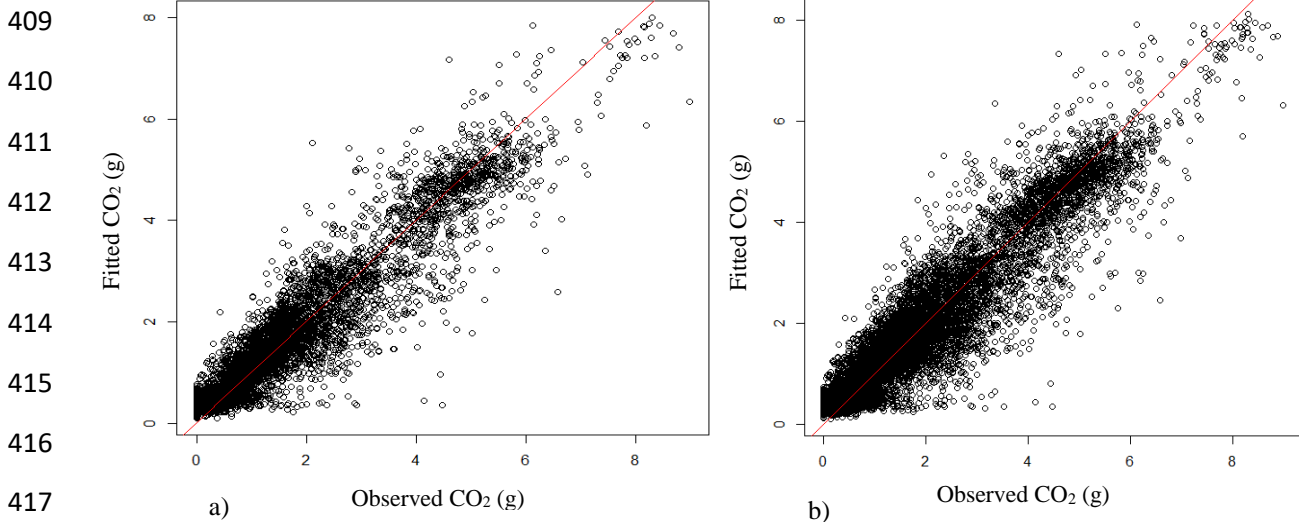
392 *Figure 9: NO<sub>x</sub>, vehicle A: a) smooth function of speed, b) smooth function of acceleration and c) smooth function of interaction between speed and acceleration*



403 *Figure 10: NO<sub>x</sub>, vehicle B: a) smooth function of speed, b) smooth function of acceleration and c) smooth function of interaction between speed and acceleration*

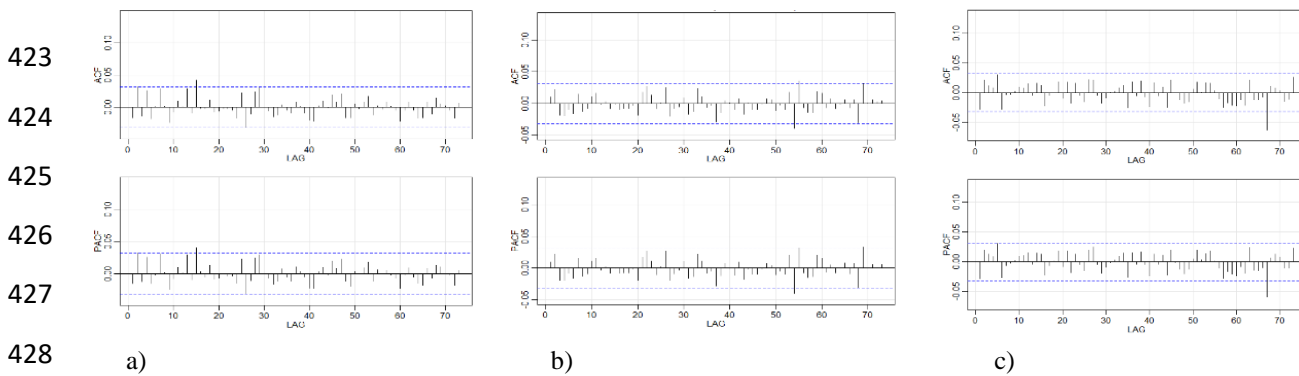
404 CO<sub>2</sub> observation (real) against fitted values for vehicle A and B are shown in Figure 11. The  
 405 reference red line indicates the case in which the fitted would be the same as the observed  
 406 values. The points are well located along this line, indicate the ability of the GAMLSS model  
 407 for estimation.

408



418 *Figure 11: fitted against observations for CO<sub>2</sub>: a) vehicle A and b) vehicle B*

419 Autocorrelation function (ACF) and partial autocorrelation function (PACF) were used to  
 420 check the structure of the residuals. These functions for vehicle A are presented in Figure 12,  
 421 that indicate clear residuals (white noise) for all the GAMLSS emission models. The ACF and  
 422 PACF of the vehicle B show the same result as well.



429 *Figure 12: ACF and PACF of the residuals for GAMLSS emission model (vehicle A): a) CO<sub>2</sub>, b) CO and c) NO<sub>x</sub>*

430 5.3. Evaluation

431 Two of the most common approaches for emission modelling are selected for comparison with  
 432 the GAMLSS emission model. These approaches are:

- 433 • Generalized Linear Model (GLM)

434 Multiple linear regression with different explanatory variables as well as GLM are widely used  
 435 in the literature for emission modelling. Here the GLM model with log link function and log-  
 436 normal distribution for the response variable is used; this model is defined by:

$$437 \quad \boldsymbol{\mu} = \exp(\mathbf{X}\boldsymbol{\gamma}), \quad \mathbf{X} = \begin{bmatrix} 1 & v_1 & v_1^3 & a_1 v_1 \\ \vdots & & \ddots & \\ 1 & v_n & v_n^3 & a_n v_n \end{bmatrix} \quad (14)$$

438 where  $\boldsymbol{\mu} = (\mu_1, \dots, \mu_n)^T$  is the  $n$ -vector of estimated mean values for the  $n$  observations,  $\mathbf{X}$  is  
 439 the design matrix of explanatory variables, and  $\boldsymbol{\gamma} = (\gamma_0, \gamma_1, \dots, \gamma_5)^T$  is the vector of parameters  
 440 including constant.

- 441 • CADI classified model

442 Using driving mode: cruise, acceleration, deceleration and idling, to explain tailpipe emission  
 443 during different traffic situations is the common classification in the emission models. This  
 444 approach is described in section 2.2. The model (2) is applied to the dataset to evaluate the  
 445 results.

446 Table 4 shows the results of the evaluation. The GLM and CADI classified model were applied  
 447 to the dataset and for each vehicle and emission type, degree of freedom, BIC and log-  
 448 likelihood ( $L$ ) are reported. The effective degree of freedom  $e$  is calculated for GAMLSS  
 449 models (Wood, 2017), which can be interpreted as an estimate of how many free parameters  
 450 are needed to represent the spline. Due to penalization, the effective degrees of freedom, which

451 indicates the amount of non-linearity of the spline, may not be integer. If the effective degrees  
 452 of freedom for a certain spline is (close to) 1, this means that the function is (close to) linear,  
 453 whilst a greater value means that the function has a greater degree of non-linearity.

454 Substantially lower values of BIC were achieved in the GAMLSS model compared to the GLM  
 455 and CADI classified approach. This indicates the strong advantage of adopting GAMLSS  
 456 formulation in modelling emissions.

457 *Table 4: BIC of the GAMLSS, GLM and CADI models with measures of their free parameters*

CO <sub>2</sub>							
Vehicle	GAMLSS			GLM (df=5)		CADI (df=32)	
	edf <i>e</i>	$\mathcal{L}$	BIC	$\mathcal{L}$	BIC	$\mathcal{L}$	BIC
A	58.2	-1241	2970	-3643	7304	-3584	7397
B	97.4	-1933	4727	-6171	12387	-6507	13258

CO							
Vehicle	GAMLSS			GLM (df=5)		CADI (df=32)	
	edf <i>e</i>	$\mathcal{L}$	BIC	$\mathcal{L}$	BIC	$\mathcal{L}$	BIC
A	63.8	31540	-62543	7907	-15733	7953	-15676
B	102.8	47256	-93603	28142	-56240	28498	-56751

NO <sub>x</sub>							
Vehicle	GAMLSS			GLM (df=5)		CADI (df=32)	
	edf <i>e</i>	$\mathcal{L}$	BIC	$\mathcal{L}$	BIC	$\mathcal{L}$	BIC
A	53.7	33844	-67234	25112	-50183	25257	-50284
B	63.2	32808	-65062	23516	-46988	23194	-46143

458

459 To complete the evaluation process, the ACF and PACF of the residuals of the GLM and CADI  
 460 classified models were investigated. The strongly significant serial correlation shown by this  
 461 shows that the residuals are not white noise and hence indicate that the systematic part of these  
 462 models is insufficient to capture all the structure. One example of these plots is shown in  
 463 Figure 13 for CO<sub>2</sub>.



464  
465  
466  
467  
468  
469  
470  
471  
472  
473  
474  
475  
476  
477  
478  
479  
480  
481  
482  
483  
484  
485  
486  
487  
488  
489  
490

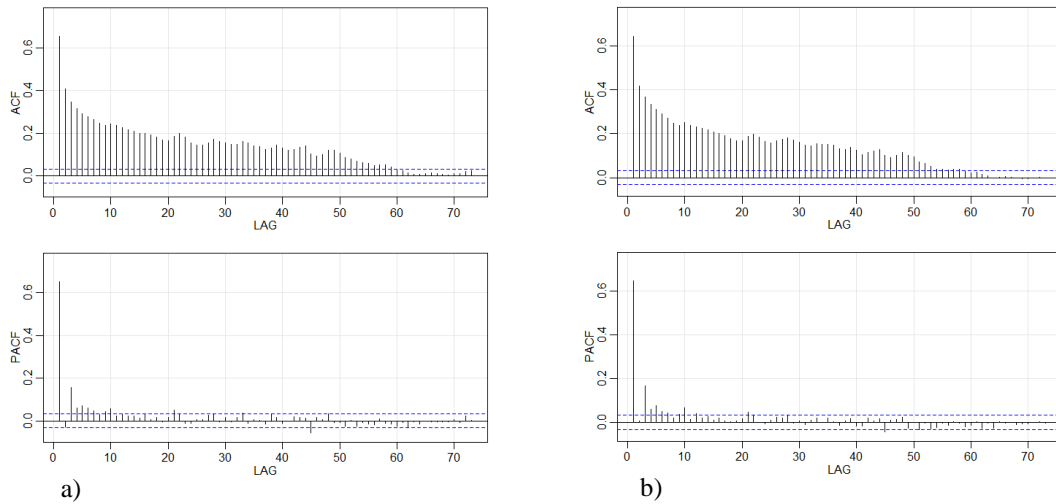


Figure 13: ACF and PACF of the residuals, vehicle 1, CO<sub>2</sub>: a) GLM model and b) CADI classified model

#### 5.4. Cross-Validation

Using a same dataset for evaluating the performance of a model as was used for fitting will usually have an unduly optimistic result. To avoid this, cross-validation (CV) procedures were developed in the early 1930s. In the CV, the statistical performance of the model is tested on a dataset that was not used in fitting it, hence giving a better understanding about the model capabilities [20].

In most cases, limitation of the available data is an issue. This leads to the idea of splitting the available data, part for fitting the model and the remainder for evaluating its performance. In this paper, the K-fold cross-validation approach is used to evaluate the performance of the GAMLSS model independent from fitting. In this procedure, the data is partitioned into K subsets or folds, each one of which is excluded in turn from the fitting dataset and then used for model validation as an independent test dataset. This leads to a total of K fitting and testing analysis in which each observation is used K-1 time in fitting and once in evaluation. Because the dataset of this study is a time series, two distinct approaches for partitioning the dataset are implemented: in the first one, the dataset is partitioned randomly without respect to the time order, while in the second approach, the time dependency of the dataset is considered by partitioning according to whole sections of the driving cycle.

491 • Random partitioning

492 The dataset was divided into 10 subsets randomly. In this procedure, each observation is used  
 493 in a test set exactly once and in a training dataset 9 times. This approach fragments the time  
 494 series of the data, so any advantage implicit in this due to temporal continuity of speed is  
 495 reduced in fitting and largely eliminated in testing.

496 The test results for 10-fold cross-validation of vehicle A are presented in Table 5. In this table  
 497 the test number shows that which of the subsets are used for the test (hence the others are used  
 498 for fitting the model). The root mean square error (RMSE)  $s$  for each test is calculated by:

$$499 \quad s = \sqrt{\frac{1}{n'} \sum_{i=1}^{n'} (y_i - \hat{y}_i)^2} \quad (8)$$

500 where  $n'$  is the number of observations in each fold (here  $n' = \frac{n}{10}$  and  $n = 7860$  is the total  
 501 number of observations),  $y$  is the observed emission and  $\hat{y}$  is the estimated emission from the  
 502 model fitted to the dataset complement of the fold.

503 *Table 5: 10-fold cross validation for vehicle A, random partitioning*

Test number	RMSE $s$ (mg/s)			$R^2$		
	CO <sub>2</sub>	CO	NO <sub>x</sub>	CO <sub>2</sub>	CO	NO <sub>x</sub>
1	420.7	20.25	0.285	0.83	0.75	0.63
2	435.9	22.58	0.279	0.88	0.78	0.68
3	435.9	22.14	0.288	0.84	0.79	0.63
4	424.3	20.74	0.286	0.87	0.78	0.61
5	412.3	20.49	0.279	0.88	0.79	0.68
6	424.3	22.14	0.275	0.86	0.69	0.71
7	489.9	21.21	0.276	0.85	0.75	0.62
8	883.2	22.80	0.289	0.36	0.63	0.59
9	433.6	22.80	0.285	0.86	0.72	0.53
10	430.1	22.14	0.283	0.85	0.68	0.63
Average	479.0	21.75	0.283	0.81	0.74	0.63

504 • Time series partitioning

506 Each of the 9 driving cycle (described in Table 1) is considered as a subset (fold) for CV. In  
 507 each test, one of the driving cycles is held-out and a model is fitted to the remaining ones. The

508 hold-out driving cycle is then used for model evaluation. This systematic approach retains the  
 509 time series structure in both the fitting and the testing dataset.

510 Each fold is used in a test exactly once and in the training dataset 8 times. The RMSE (Equation  
 511 8) is used as an evaluation score for each test. It should be noted that the number of observations  
 512 in each driving cycle ( $n'$ ) is varies among different cycles. The results of time series  
 513 cross- validation for vehicle A are presented in Table 6.

514 *Table 6: 10-fold cross validation for vehicle A, time series partitioning*

Test number	Driving cycle	RMSE $s$ (mg/s)			$R^2$		
		CO <sub>2</sub>	CO	NO <sub>x</sub>	CO <sub>2</sub>	CO	NO <sub>x</sub>
1	Urban-Free flow	468.2	20.48	0.261	0.85	0.78	0.65
2	Urban-AM peak	473.1	21.15	0.259	0.89	0.74	0.66
3	Urban-Inter peak	471.2	22.01	0.255	0.84	0.77	0.64
4	Suburban-Free flow	432.1	19.63	0.244	0.87	0.76	0.67
5	Suburban-AM peak	449.2	19.33	0.245	0.85	0.77	0.63
6	Suburban-Inter peak	437.3	19.67	0.24	0.84	0.75	0.65
7	Motorway-Free flow	461.3	21.22	0.274	0.87	0.79	0.64
8	Motorway-AM peak	478.3	20.98	0.265	0.86	0.71	0.66
9	Motorway-Inter peak	475.6	20.87	0.271	0.85	0.76	0.65
Average		460.7	20.60	0.257	0.86	0.74	0.65

523 In addition to that, the same procedure is applied on the 3 driving cycles (folds) instead of 9:  
 524 three different traffic conditions (Free flow, AM peak, Inter peak) in each road type are added  
 525 together to have the urban, suburban and motorway driving cycles (folds). The results of RMSE  
 526 for each fold is presented in Table 7. This table shows that the suburban driving cycle has the  
 527 lowest average RMSE compared to urban and motorway road types. This emphasises the  
 528 importance of including urban and motorway driving cycles in emission modelling compared  
 529 to the suburban ones.

530 *Table 7: average RMSE in urban, suburban and motorway driving cycles*

Driving cycle	Average RMSE $s$ (mg/s)		
	CO <sub>2</sub>	CO	NO <sub>x</sub>
Urban	470.8	21.21	0.258
Suburban	439.5	19.54	0.243
Motorway	471.73	21.02	0.270

534 The average of the RMSE results for random and time series CV are presented in Table 8. In  
 535 this table, corresponding fitting results for the full models (GAMLSS, GLM and CADI) are  
 536 presented as well.

537 *Table 8: Fitting results of models for Vehicle A on the full dataset*

		RMSE $s$ (mg/s)			$R^2$		
		CO <sub>2</sub>	CO	NO <sub>x</sub>	CO <sub>2</sub>	CO	NO <sub>x</sub>
Cross-validation	Random CV	479.0	21.75	0.283	0.81	0.74	0.63
	Time series CV	460.7	20.60	0.257	0.86	0.74	0.65
Model (fitted to the whole dataset)	GAMLSS	443.8	16.43	0.228	0.87	0.85	0.76
	GLM	603.3	26.32	0.413	0.76	0.61	0.21
	CADI	563.9	24.90	0.363	0.79	0.65	0.39

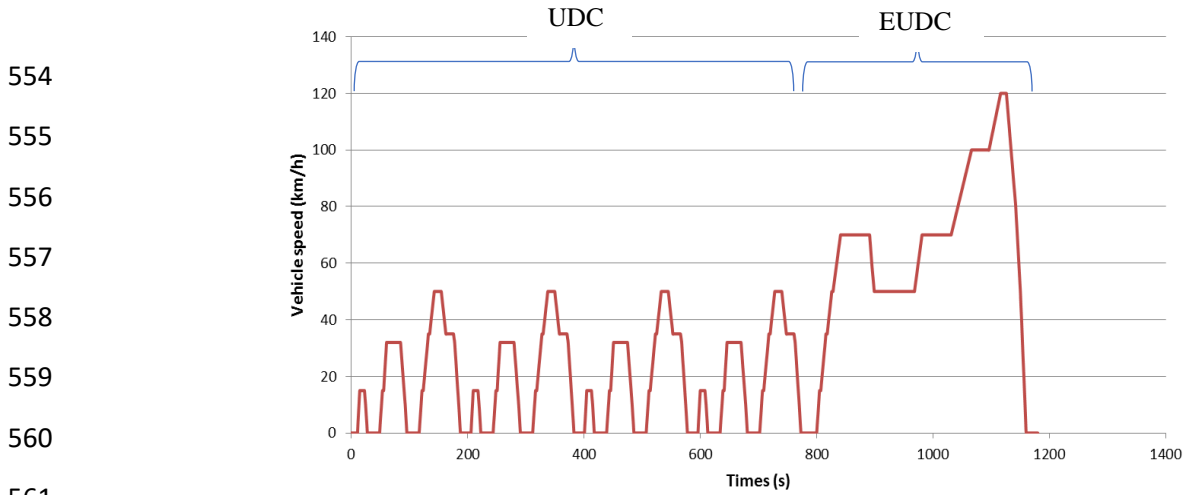
538

539 The results of CV approaches show that splitting the dataset without respect to the time series  
 540 (random) is a stricter approach than time series partitioning, leading to an average of the RMSE  
 541 that is slightly lower: 3.8%, 5.22% and 8.98% lower in CO<sub>2</sub>, CO and NO<sub>x</sub>, respectively. in  
 542 addition, comparison CV results with the fully fitted GAMLSS model shows that although  
 543 these results are somewhat weaker than the corresponding fully fitted ones, they remain  
 544 preferable to the GLM and CADI even when those are fully fitted. The GAMLSS model out-  
 545 performs the GLM and CADI models for each of the three emissions when fitted to the full  
 546 dataset.

547 [5.5. Prediction for NEDC driving cycle](#)

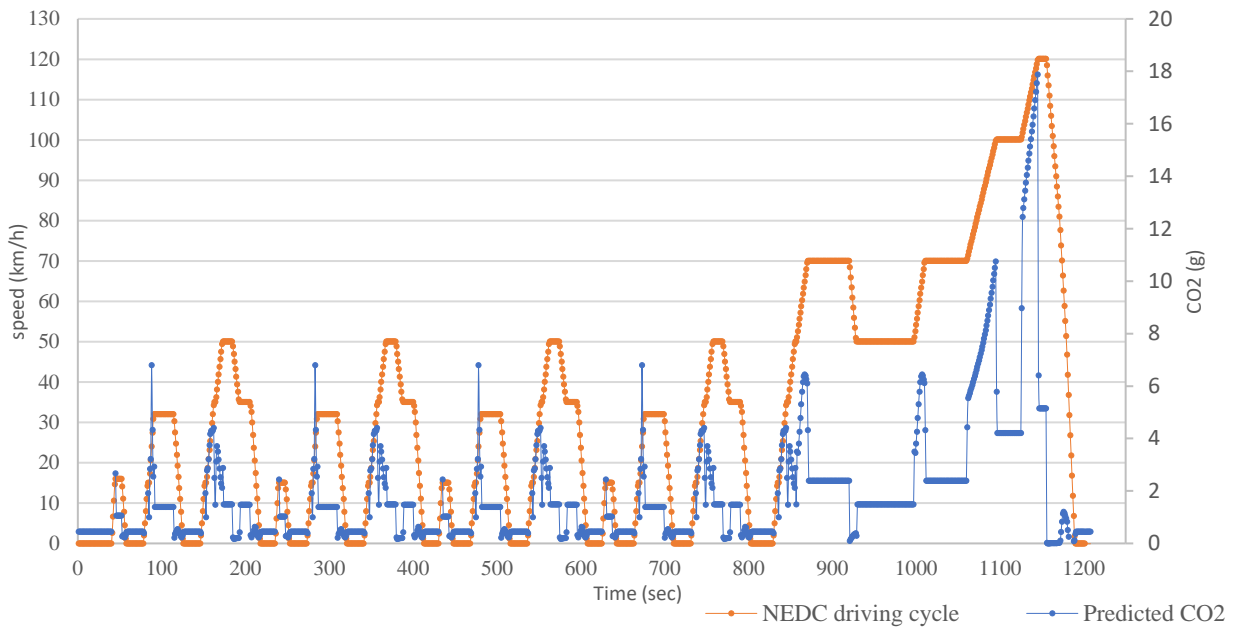
548 To show the intended use of the developed method for prediction, the GAMLSS model is  
 549 applied for NEDC driving cycle. NEDC was used as the reference cycle for emission tests of  
 550 vehicles until Euro 6, in Europe and some other countries. As it is shown in Figure 14, it  
 551 contains an Urban Driving Cycle part (UDC) that is repeated four times, and an Extra-Urban  
 552 Driving cycle part (EUDC) after that.

553



562 *Figure 14: New European Driving Cycle (NEDC) [21]*

563 As an example application, the model for vehicle 1 is applied to predict the CO<sub>2</sub> values of this  
 564 vehicle while following the NEDC driving cycle (Figure 15).



565 *Figure 15: predicted CO<sub>2</sub> values for NEDC driving cycle*

566 The total CO<sub>2</sub> emission per kilometre of NEDC driving cycle for this vehicle type is reported  
 567 as 110 g/km. GAMLSS approach estimation is 115 g/km, which therefore represents good  
 568 agreement with the reported emission.

## 569 6. Summary and Conclusion

570 This paper presents a novel statistical approach to build a vehicle emission model, that can  
571 describe the relationship between vehicle movements variables, speed and acceleration, with  
572 tailpipe emission. Speed, acceleration and their interaction are the explanatory variables of this  
573 model. Cubic smoothing spline function of these variables are added together to build a general  
574 additive model for location, scale and shape. In this form of model, the error structure is  
575 allowed to extend beyond the exponential family of distributions, hence, more flexible  
576 distributions can be fitted.

577 To evaluate these GAMLSS emission models, BIC values of that are compared with GLM and  
578 CADI classified model. The results indicate the substantial advantage of this model over GLM  
579 and CADI classified model. A 10-fold cross-validation approach was used to test the models.  
580 To show the ability of the model to predict emission from a driving cycle, CO<sub>2</sub> emission values  
581 are predicted with this model for NEDC driving cycle.

582 The reason of using cubic smoothing spline is that it offers greater flexibility in following the  
583 shape of the relationship between the explanatory variables and the emissions. The generalized  
584 linear or classified models are insufficient to describe the relationship between explanatory  
585 variables and emission, as shown by the figures of smooth splines of speed and acceleration,  
586 which indicate that this is more complicated. Furthermore, there is no requirement to classify  
587 vehicle operation regimes in this approach, as all variations can be estimated by a single model.

## 588 Acknowledgment

589 This research was funded by the Lloyd's Register Foundation (LRF), which helps to protect  
590 life and property by supporting engineering-related education, public engagement and the

591 application of research. The vehicle emission dataset is provided by the Transport for London  
592 (TfL).

## 593 References

- 594 [1] J. L. Jimenez-Palacios, "Understanding and Quantifying Motor Vehicle Emissions with Vehicle Specific Power and  
595 TILDAS Remote Sensing," PhD, Mechanical Engineering Massachusetts Institute of Technology, 1999.
- 596 [2] G. Boutler, S. McCrae, and T. Barlow, "A review of instantaneous emission models for road vehicles ", Transport  
597 Research Laboratory (TRL), No. 323-R041 ,2007.
- 598 [3] L. L. John Koupal, Edward Nam, James Warila, Carl Scarbro, Edward Glover, Robert Giannelli, "MOVES2004  
599 Energy and Emission Inputs," *U.S. Environmental Protection Agency, Office of Transportation and Air Quality*, vol.  
600 Report EPA420-P-05-003, March 2005.
- 601 [4] R. Smit, R. Smokers, and E. Rabé, "A new modelling approach for road traffic emissions: VERSIT+," *Transportation  
602 Research Part D: Transport and Environment*, vol. 12, pp. 414-422, 8// 2007.
- 603 [5] K. Ahn, H. Rakha, A. Trani, and M. Van Aerde, "Estimating Vehicle Fuel Consumption and Emissions based on  
604 Instantaneous Speed and Acceleration Levels," *Journal of Transportation Engineering*, vol. 128, pp. 182-190,  
605 2002/03/01 2002.
- 606 [6] H. Rakha, K. Ahn, and A. Trani, "Development of VT-Micro model for estimating hot stabilized light duty vehicle  
607 and truck emissions," *Transportation Research Part D: Transport and Environment*, vol. 9, pp. 49-74, 1// 2004.
- 608 [7] H. Rakha and K. Ahn, "Integration Modeling Framework for Estimating Mobile Source Emissions," *Journal of  
609 Transportation Engineering*, vol. 130, pp. 183-193, 2004/03/01 2004.
- 610 [8] A. Cappiello, I. Chabini, E. K. Nam, A. Lue, and M. A. Zeid, "A statistical model of vehicle emissions and fuel  
611 consumption," in *Proceedings. The IEEE 5th International Conference on Intelligent Transportation Systems*, 2002,  
612 pp. 801-809.
- 613 [9] F. An, M. Barth, J. Norbeck, and M. Ross, "Development of Comprehensive Modal Emissions Model: operating  
614 under hot-stabilized conditions," *Transportation research Record* vol. 1586, pp. 52-62, 1997.
- 615 [10] F. A. Matthew Barth, Younglove T, Scora G, Levine C, Ross M and Wenzel T, "Development of a comprehensive  
616 modal emissions model " NCHRP Project 25-11 Project 25-11, April 2000.
- 617 [11] B. Scora "Comprehensive Modal Emissions Model (CMEM)," University of California, Riverside, Center for  
618 Environmental Research and Technology 2006.
- 619 [12] "Chasis Dynamometer test procedures for approval of low emission adaptations " Clean Air Zone (CAZ)- Clean  
620 vehicle retrofit certification (CVRC), Version 4 ,August 2017
- 621 [13] R. A. Rigby and D. M. Stasinopoulos, "Generalized additive models for location, scale and shape," *Journal of the  
622 Royal Statistical Society: Series C (Applied Statistics)*, vol. 54, pp. 507-554, 2005.
- 623 [14] G. Marra and R. Radice, "Bivariate copula additive models for location, scale and shape," *Computational Statistics  
624 & Data Analysis*, vol. 112, pp. 99-113, 2017/08/01/ 2017.
- 625 [15] S N Wood, *Generalized Additive Models: an introduction with R* CRS Press 2017
- 626 [16] S. N. Wood. (2018). *mgcv: Mixed GAM computation vehicle with automatic smoothness estimation*. Available:  
627 URL <http://CRAN.R-project.org/package=mgcv>
- 628 [17] G. Marra and R. Radice. (2018). *GJRM: Generalized Joint Regression Modelling*. Available: URL [http://CRAN.R-](http://CRAN.R-project.org/package=GJRM)  
629 [project.org/package=GJRM](http://CRAN.R-project.org/package=GJRM)
- 630 [18] J. Duchon, "Splines minimizing rotation-invariant semi-norms in Sobolev spaces," in *Constructive Theory of  
631 Functions of Several Variables*, Berlin, Heidelberg, 1977, pp. 85-100.
- 632 [19] R. A. Rigby and D. M. Stasinopoulos, "Generalized additive models for location, scale and shape," *Journal of the  
633 Royal Statistical Society: Series C (Applied Statistics)*, vol. 54, pp. 507-554, 2005.
- 634 [20] S. Arlot and A. Celisse, "A survey of cross-validation procedures for model selection," *Statist. Surv.*, vol. 4, pp. 40-  
635 79, 2010 2010.
- 636 [21] T. J. Barlow, S. Latham, I. S. McCrae, and P. G. Boulter, "A reference book of driving cycles for use in the  
637 measurement of road vehicle emissions " TRL2009.

638

## 639 Appendix: R codes for GAMLSS emission model

640 The R codes for building GAMLSS emission model for vehicle type A and emission type CO<sub>2</sub>  
641 is presented here. The data frame “V.1” includes: “coo.v1” “s.v1” and “a.v1” that representing  
642 CO<sub>2</sub>, speed and acceleration for vehicle A, respectively.

```
643 >library(mgcv)
644 >library(GJRM)
645 >library(astsa)
646 >library(xlsx)
647 >V.1 <- read.xlsx("V.1.xlsx") #load the data from excel file for vehicle
648 1
649 >V.1 <- as.data.frame(V.1)
650 >f11.coo.v1 <- list(coo.v1 ~ s(s.v1) + s(acce.v1) + ti(s.v1, a.v1), #define the systematic part of the
651 model
652 ~ s(s.v1) + s(a.v1) + ti(s.v1, a.v1) )
653 >Fisk.coo.v1 <- gamlss(f11.coo.v1, data = V.1, margin = "FISK") #build the GAMLSS emission model with Fisk
654 distribution
655 > post.check(Fisk.coo.v1) #check the selected distribution
656 > summary(Fisk.coo.v1) #summary of the model
657 >plot(Fisk.coo.v1, eq = 1, scale = 0, pages = 1, scheme = 1) #plot the fitted model based on the first
658 equation (Location)
659 >plot(Fisk.coo.v1, eq = 2, scale = 0, pages = 1, scheme = 1) #plot the fitted model based on the
660 second equation (Scale)
661 >pred.Fisk.coo.v1 <- pred.mvt(Fisk.coo.v1, fun = "mean", n.sim = 100, prob.lev = 0.05, newdata = V.1) #use the model
662 for estimation
663 >acf2( V.1$coo.v1 - pred.Fisk.coo.v1$pred) #plot acf/pacf of the residuals
664
665 >plot(V.1$coo.v1, pred.Fisk.coo.v1$pred) #plot fitted against observations
666
```